This journal is © The Royal Society of Chemistry 2013

Supporting Information:

Block Copolymer-Ferroelectric Nanoparticle Nanocomposites

Xinchang Pang,[a] Yanjie He,[a] Beibei Jiang,[a] James Iocozzia,[a] Lei Zhao,[a] Hanzheng Guo,[b] Jin Liu,[b] Mufit Akinc,[b] Nicola Bowler,[b] Xiaoli Tan,[b] and Zhiqun Lin[a]*

[a]School of Materials Science and Engineering, Georgia Institute of Technology, Atlanta, GA 30332, USA

[b]Department of Materials Science and Engineering, Iowa State University, Ames, Iowa 50011, USA

* To whom correspondence should be addressed. Email: zhiqun.lin@mse.gatech.edu

Table S1. Molecular weights of amphiphilic star-like PAA-*b*-PS diblock copolymers.[1]

Entry	$M_{n,\,PAA}$[a]	$M_{n,\,PS}$[b]	M_w/M_n[c]
Sample-1	4,500	4,100	1.13
Sample-2	8,400	5,200	1.10
Sample-3	28,100	29,680	1.18

[a]Number average molecular weight, M_n of each PAA block calculated from the molecular weight difference between P*t*BA block (before hydrolysis) and PAA block (after hydrolysis) based on ^{1}H-NMR spectra. [b]M_n of each PS arm calculated from ^{1}H NMR data.[c]Polydispersity index, PDI determined by GPC.

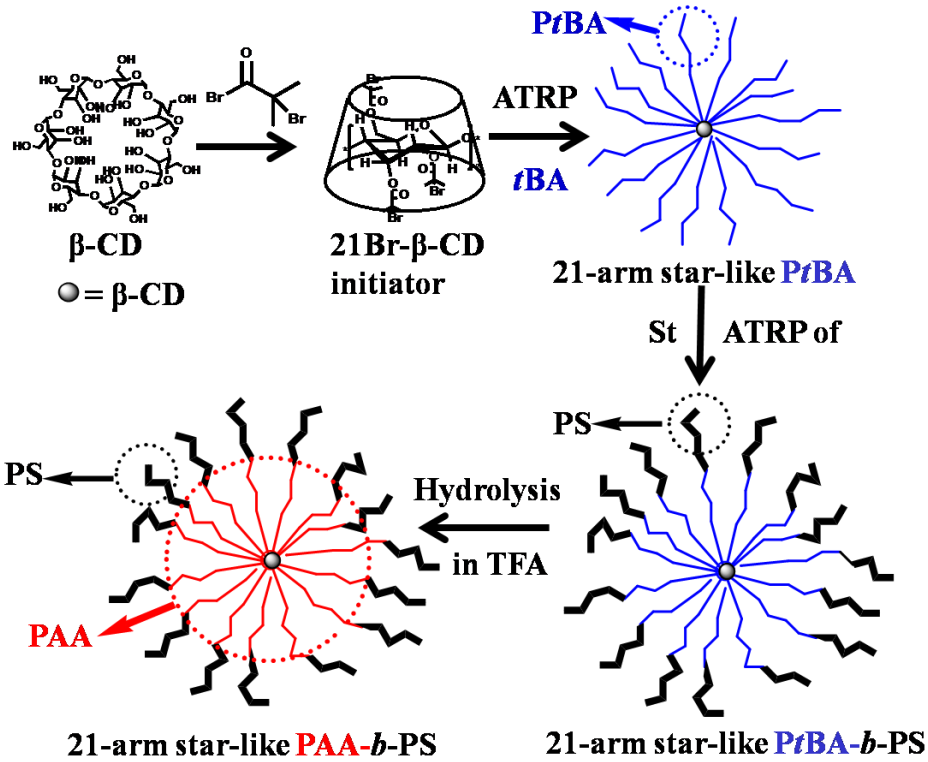

Scheme S1. Schematic representation of the synthesis of amphiphilic star-like PAA-*b*-PS diblock copolymers by sequential atom transfer radical polymerization (ATRP) of *tert*-butyl acrylate and styrene.[1]

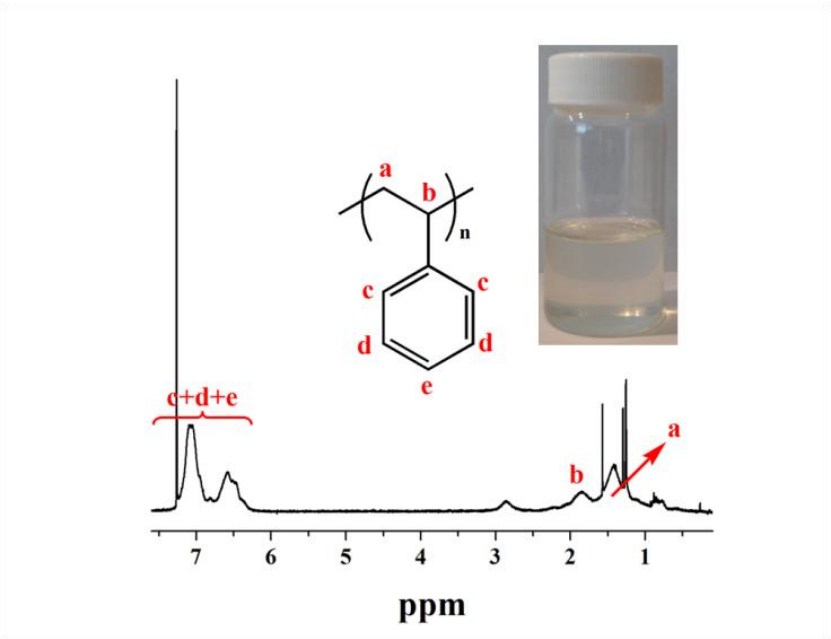

Figure S1. ^{1}H -NMR spectrum of $BaTiO_3$ permanently capped with PS chains (sample-a, *D* = ~6 nm, solvent: $CDCl_3$). Inset: digital image of PS-functionalized $BaTiO_3$ NP toluene solution (*c*= 10mg/mL).

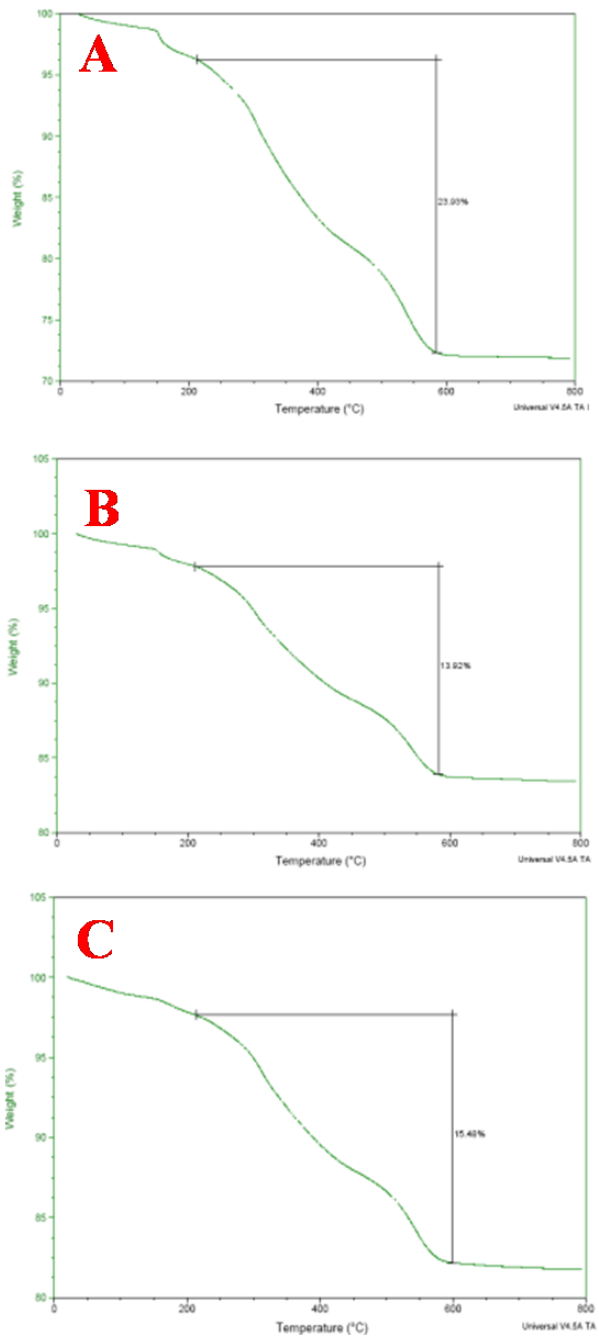

Figure S2. (A-C) The thermogravimetric analysis of PS-functionalized $BaTiO_3$ NPs with different sizes by using different star-like PAA-*b*-PS as templates (i.e., sample-1, sample-2, and sample-3 in Table S1, respectively).Weight fractions of polymers are 23.93 % in A (*D* = ~6 nm); B=13.92 % (*D* = ~11 nm); and C=15.48 % (*D* = ~27 nm).

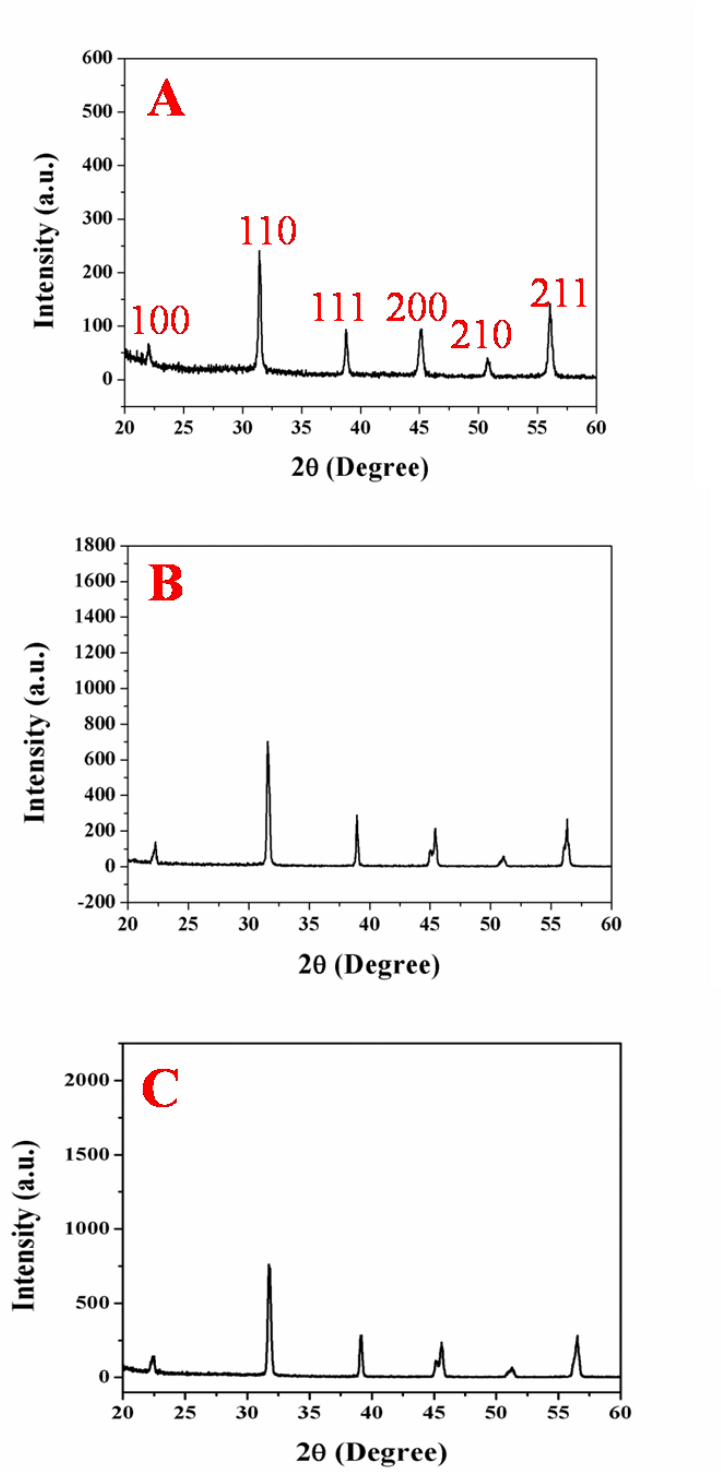

Figure S3. (A-C) XRD patterns of PS-functionalized $BaTiO_3$ NPs with different sizes by using different star-like PAA-*b*-PS as templates (i.e., sample-1, sample-2and sample-3 in Table S1, respectively). The diameters of NPs are D = ~6 nm in A; D = ~11 nm in B; and D = ~27 nm in C.

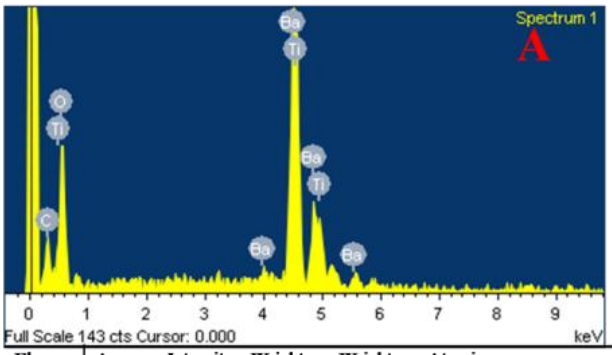

Element	App Conc.	Intensity Corrn.	Weight %	Weight % Sigma	Atomic %
CK	33.47	1.0106	6.25	1.23	8.67
OK	92.09	0.7996	21.74	2.16	48.73
TiK	148.33	0.9905	28.26	1.95	21.17
BaL	206.58	0.8912	43.75	2.68	21.43
Totals			100.00		

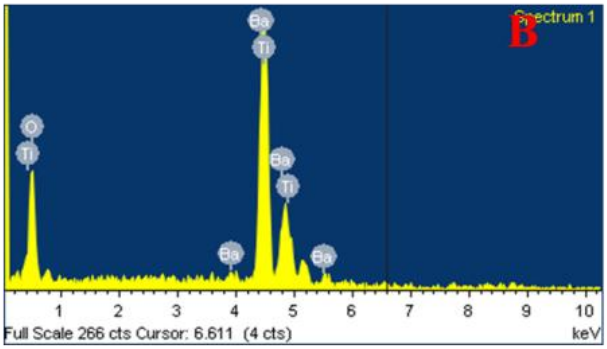

Element	Weight%	Atomic%
OK	21.19	58.51
TiK	29.78	20.99
BaL	49.03	20.50
Totals	100.00	

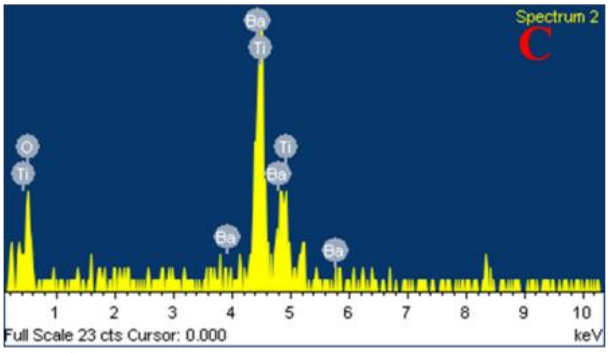

Element	App Conc.	Intensity Corrn.	Weight%	Weight% Sigma	Atomic%
OK	5.39	0.9554	18.48	6.03	55.65
TiK	7.64	1.0414	24.04	6.53	24.18
BaL	16.44	0.9375	57.48	8.55	20.17
Totals			100.00		

Figure S4. (A-C) EDS spectra of PS-functionalized $BaTiO_3$ NPs with different sizes by using different star-like PAA-*b*-PS as templates (i.e., sample-1, sample-2, and sample-3 in Table S1, respectively). The diameters of NPs are D = ~6 nm in A; D = ~11 nm in B; and D = ~27 nm in C.

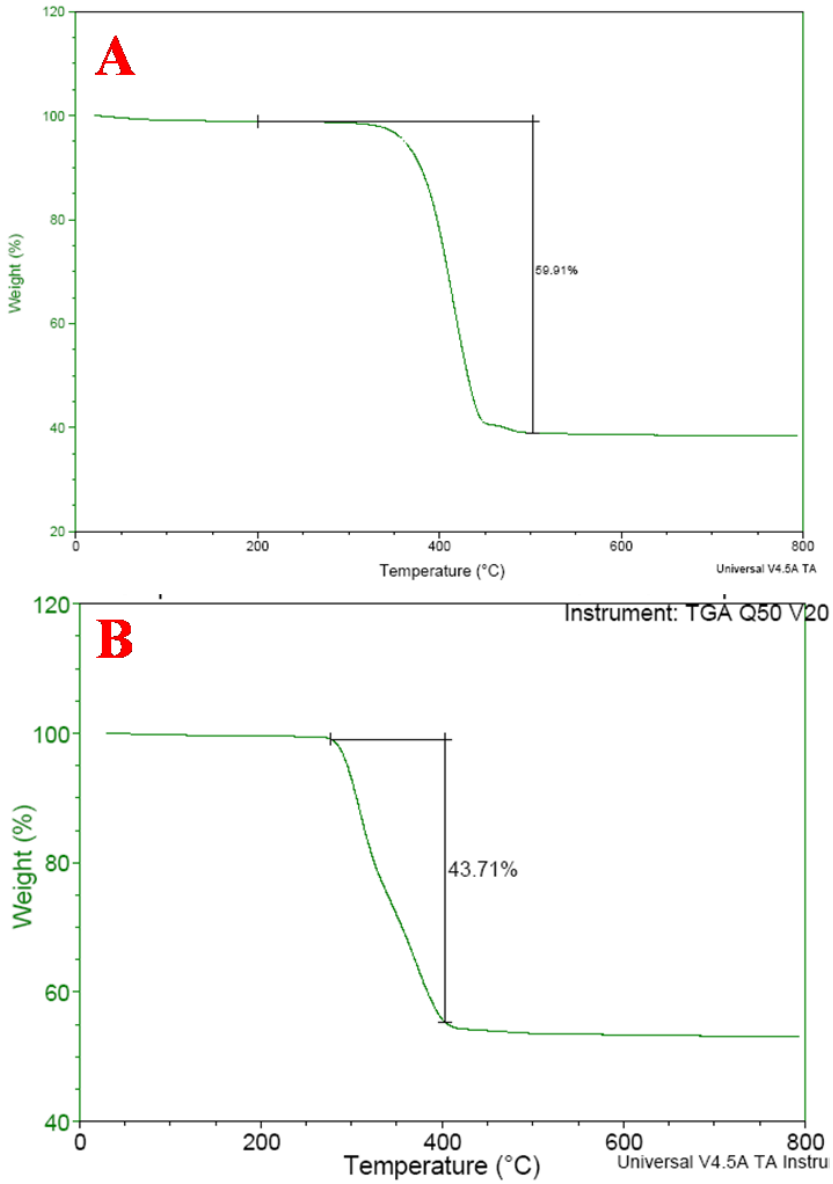

Figure S5. The thermogravimetric analysis of nanocomosites by mixing PS-functionalized $BaTiO_3$ NPs (D = ~11 nm) and PS-*b*-PMMA (M_{PS}=45,900 and M_{PMMA}=138,000) at the different volume fractions of NPs: 11.5% in A and 16.3% in B.

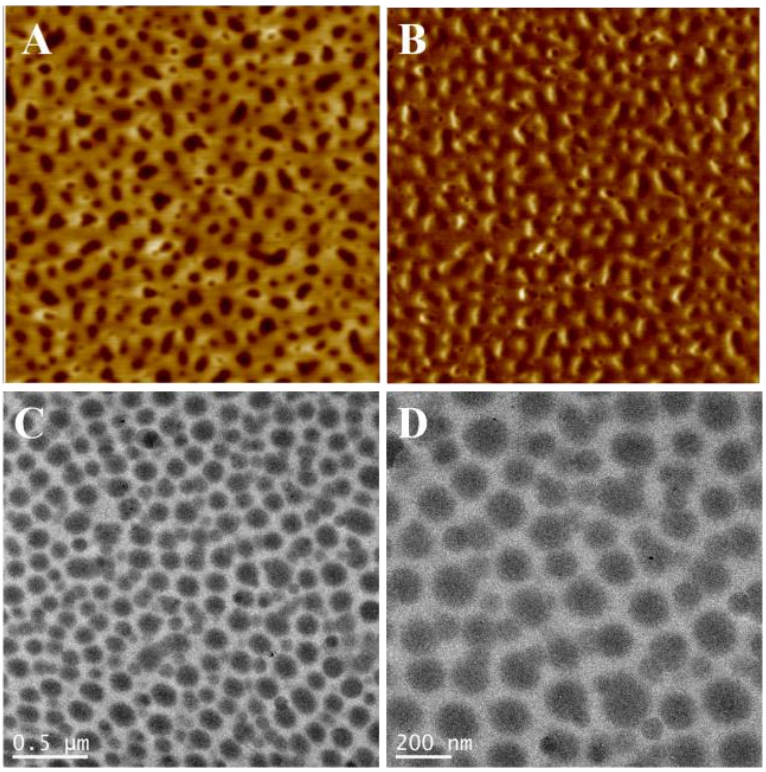

Figure S6. AFM and TEM images of pure PS-*b*-PMMA (M_{PS}=315,000 and M_{PMMA}=785,000) thin film. (A) AFM height and (B) phase images of as-prepared PS-*b*-PMMA (M_{PS}=315,000 and M_{PMMA}=785,000); image size= 10.0×10.0μm^2, Z range= 30 nm for (A) and 36.9^o for (B).

(C)-(D) TEM images of PS-*b*-PMMA thin film formed after the acetone vapor annealing for 6 h. The PS nanodomains appeared dark in the bright PMMA matrix. The average diameter of the PS nanocylinders is estimated to be 161.7±12.5 nm, obtained by using standard image analysis software *ImageJ*. The film thickness is 46 nm.

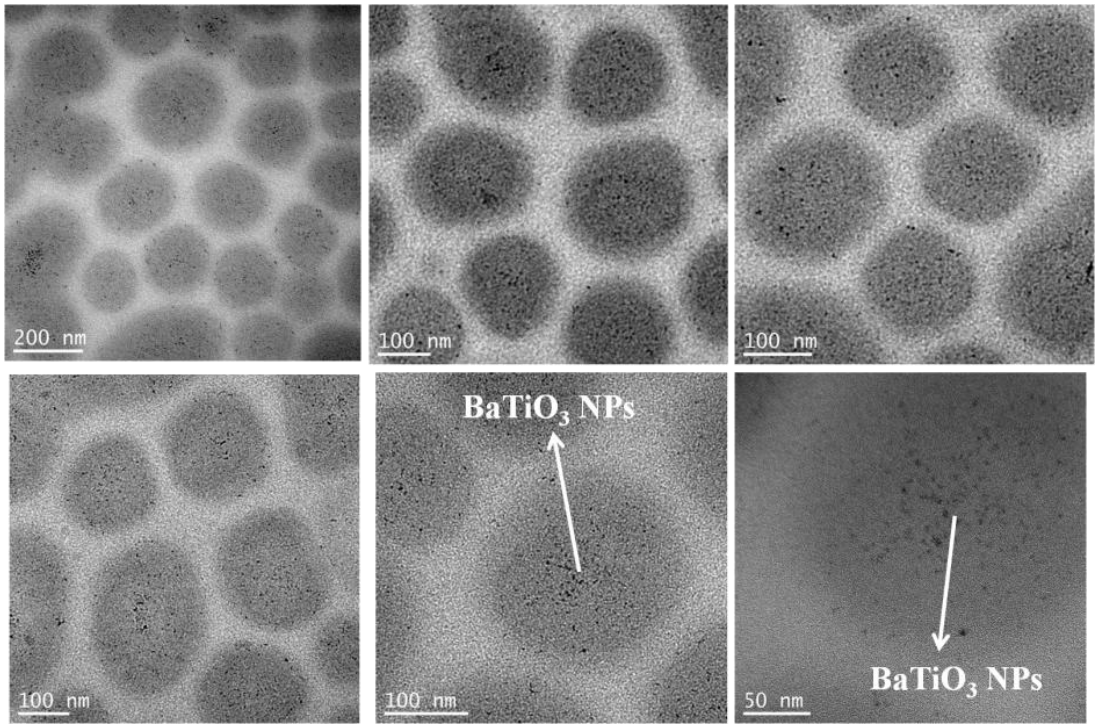

Figure S7. TEM images of thin film of PS-*b*-PMMA (M_{PS}=315,000 and M_{PMMA}=785,000)/ PS-functionalized $BaTiO_3$ NP (*D* = ~6 nm) nanocomposites formed after the acetone vapor annealing for 6h. The volume fraction of $BaTiO_3$ NPs was 10.8%. The vertically oriented arrays of PS nanodomains containing $BaTiO_3$ NPs appeared dark. The average diameter of the PS nanocylinders after the addition of $BaTiO_3$ NPs is estimated to be 206.4±31.2 nm, obtained by using standard image analysis software *ImageJ*. The film thickness is 56nm. The average number of $BaTiO_3$ NPs in the PS nanocylinders is approximately 306, calculated based on the volume fraction of $BaTiO_3$ NPs and the size of the PS nanocylinders.

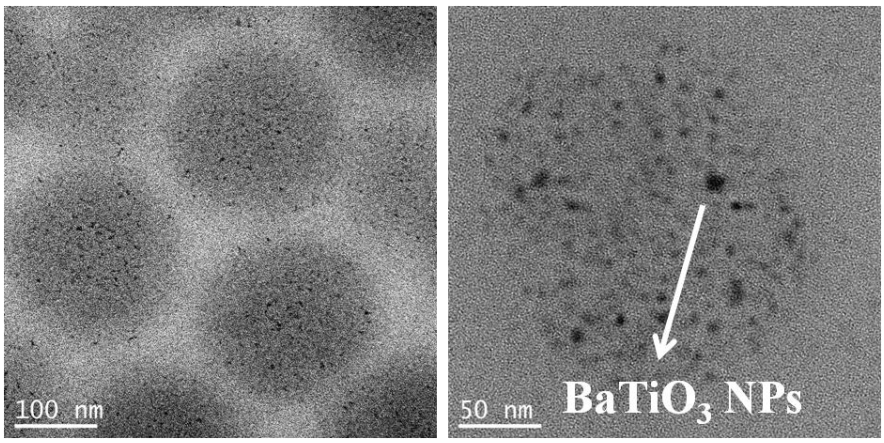

Figure S8. TEM images of thin film of PS-*b*-PMMA (M_{PS}=315,000 and M_{PMMA}=785,000)/ PS-functionalized $BaTiO_3$ NP (*D* = ~6 nm) nanocomposites formed after the acetone vapor annealing for 6h. The volume fraction of $BaTiO_3$ NPs was 16.8%. The vertically oriented arrays of PS nanodomains containing $BaTiO_3$ NPs appeared dark. The average diameter of the PS nanocylinders after the addition of $BaTiO_3$ NPs is estimated to be 220.8±25.3 nm, obtained by using standard image analysis software *ImageJ*. The film thickness is 61 nm. The average number of $BaTiO_3$ NPs in the PS nanocylinders is approximately 461, calculated based on the volume fraction of $BaTiO_3$ NPs and the size of the PS nanocylinders.

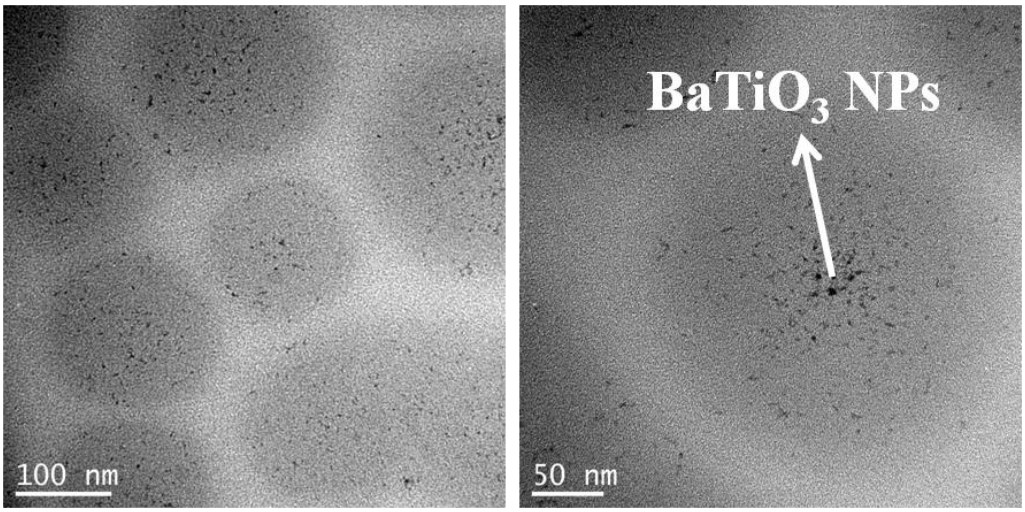

Figure S9. TEM images of thin film of PS-*b*-PMMA (M_{PS}=315,000 and M_{PMMA}=785,000)/ PS-functionalized $BaTiO_3$ NP (*D* = ~11 nm) nanocomposites formed after the acetone vapor annealing for 6h. The volume fraction of $BaTiO_3$ NPs was 15.9%. The vertically oriented arrays of PS nanodomains containing $BaTiO_3$ NPs appeared dark. The average diameter of the PS nanocylinders after the addition of $BaTiO_3$ NPs is estimated to be 218.2±28.6 nm, obtained by using standard image analysis software *ImageJ*. The film thickness is 58 nm. The average number of $BaTiO_3$ NPs in the PS nanocylinders is approximately 239, calculated based on the volume fraction of $BaTiO_3$ NPs and the size of PS nanocylinders.

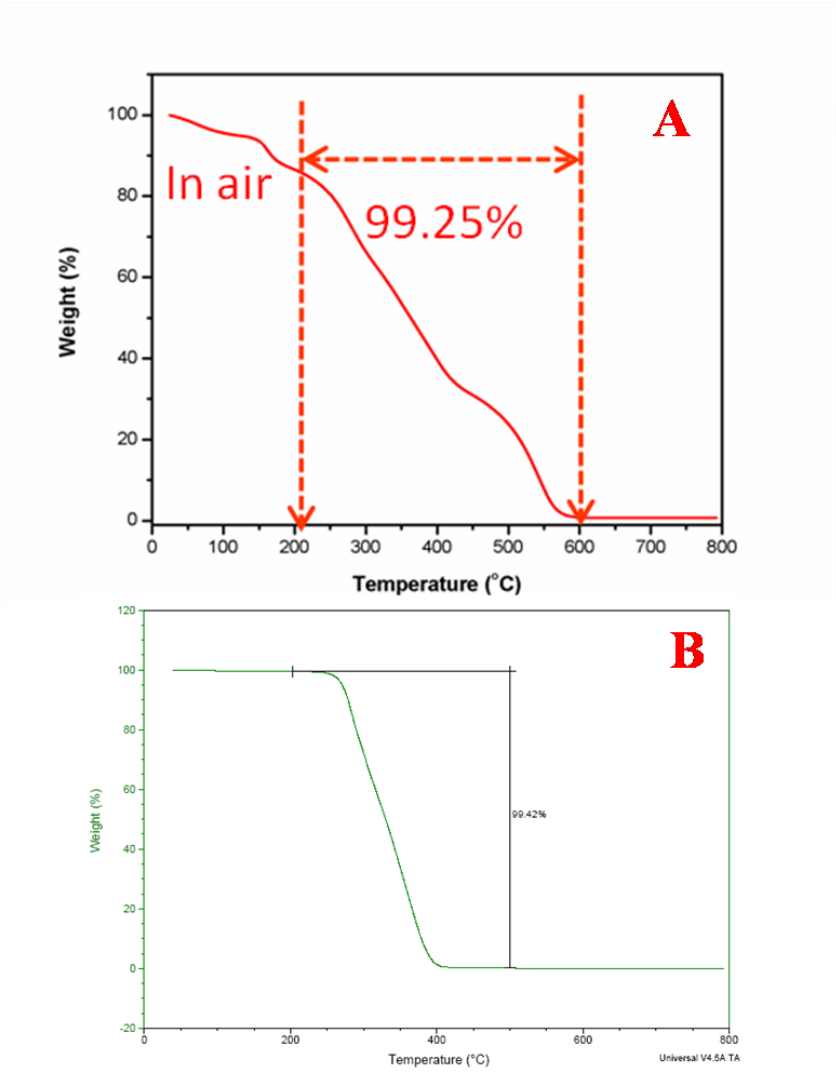

Figure S10. Thermogravimetric analysis of star-like PAA-*b*-PS (sample-1 in Table S1) and PS-*b*-PMMA (M_{PS}=45,900 and M_{PMMA}=138,000).

Reference

(1) Pang, X.; Zhao, L.; Akinc, M.; Kim, J. K.; Lin, Z. *Macromolecules*, **2011**, *44*, 3746.